

Pontryagin-Guided Deep Policy Learning for Constrained Dynamic Portfolio Choice

Jeonggyu Huh¹, Jaegi Jeon^{*2}, Hyeng Keun Koo³, and Byung Hwa Lim⁴

¹Department of Mathematics, Sungkyunkwan University, Republic of Korea

²Graduate School of Data Science, Chonnam National University, Republic of Korea

³Department of Financial Engineering, Ajou University, Republic of Korea

⁴Department of Fintech, SKK Business School, Sungkyunkwan University, Seoul, Republic of Korea

September 23, 2025

Abstract

We present a Pontryagin-Guided Direct Policy Optimization (PG-DPO) framework for *constrained* continuous-time portfolio-consumption problems that scales to hundreds of assets. The method couples neural policies with Pontryagin’s Maximum Principle and enforces feasibility via a lightweight log-barrier stagewise solve; a *manifold-projection* variant (P-PGDPO) projects controls onto the PMP/KKT manifold using stabilized adjoints. We prove a barrier-KKT correspondence with $O(\epsilon)$ policy error and $O(\epsilon^2)$ instantaneous Hamiltonian gap, and extend the BPTT-PMP match to constrained settings. On short-sale (nonnegativity, floating cash) and wealth-proportional consumption caps, P-PGDPO reduces risky-weight errors by orders of magnitude versus baseline PG-DPO, while the one-dimensional consumption control shows smaller but consistent gains near binding caps. The approach remains effective when closed-form benchmarks are unavailable, and is readily extensible to transaction costs and interacting limits—promising even greater benefits under time-varying investment opportunities where classical solutions are scarce.

1 Introduction

Dynamic portfolio choice—how an investor allocates wealth across multiple assets and consumes over time under uncertainty—has been central to modern finance since the seminal works of Samuelson (1969) and Merton (1969, 1971). Under idealized assumptions such as complete markets, frictionless trade, and unlimited shorting/borrowing, this “Merton problem” can admit elegant (semi-)closed-form solutions (e.g., Kim & Omberg, 1996; Liu, 2007). Real markets, however, impose *constraints*—short-sale bans and leverage limits, pointwise consumption bounds, and ratcheting rules—that invalidate frictionless formulas and transform the Bellman equation into variational inequalities or free-boundary problems (e.g., Karatzas et al., 1987; Cvitanić & Karatzas, 1996; Karatzas & Shreve, 1998; Shreve & Soner, 1994; Fleming & Soner, 2006; Dybvig, 1995; Constantinides, 1990; Sundaresan, 1989). At the same time, classical dynamic programming (DP) suffers acutely from the curse of dimensionality in multi-asset settings, which has historically constrained empirical and numerical studies to small portfolios even without constraints (Campbell & Viceira, 1999, 2001; Campbell et al., 2003; Balduzzi & Lynch, 1999; Lynch & Balduzzi, 2000; Lynch, 2001; Brandt et al., 2005; Buraschi et al., 2010; Garlappi & Skoulakis, 2010; Jurek & Viceira, 2011).

*Corresponding Author: jaegijeon@jnu.ac.kr

Following Huh et al. (2025), *PG-DPO* (Pontryagin-Guided Direct Policy Optimization) integrates Pontryagin’s Maximum Principle into direct, policy-centric training: neural investment/consumption policies are learned by backpropagation-through-time while adjoint (costate) signals steer updates toward Hamiltonian stationarity, thereby avoiding explicit value-function approximation and operating directly in the space of feasible controls. The companion *Projected PG-DPO (P-PGDPO)* in Huh et al. (2025) decouples adjoint estimation from control construction and computes controls by *projecting* adjoint-informed proposals onto the *PMP-optimal control manifold* via a small barrier-regularized stagewise maximization (an interior-point Newton step).

*In this paper we adapt and extend these two components to **constrained** portfolio choice.* The control manifold is augmented to encode portfolio and consumption constraints (e.g., simplex/nonnegativity for weights; box or wealth-proportional caps for consumption), the barrier links the projection to the KKT system, and the projection yields feasible, PMP-consistent controls at each time-state without high-dimensional value-function grids. Methodologically, we formalize the PMP setup and its barrier/KKT enforcement (Fleming & Soner, 2006; Pham, 2009), and—building on the unconstrained analysis of Huh et al. (2025)—establish a barrier–KKT correspondence at the stagewise Hamiltonian, prove stability of autodiff costates under manifold projection, and derive finite- ϵ error controls (policy error $O(\epsilon)$, instantaneous Hamiltonian gap $O(\epsilon^2)$) for the projection map on the feasible control manifold. Empirically, we quantify performance via policy errors, Hamiltonian first-order-condition residuals, and utility gaps, and visualize adherence to constraint boundaries.

Positioned against value-based PDE/BSDE solvers and PINNs—which typically approximate value functions or PDE solutions and become cumbersome with large state/action spaces or intricate constraints (Han et al., 2018; Weinan, 2017; Raissi et al., 2019; Dai et al., 2023)—our approach remains policy-centric: the barrier-regularized projection enforces feasibility exactly at each time-state and aligns controls with Hamiltonian stationarity. We study two canonical constraint families—constraints on portfolio weights π (e.g., nonnegativity/simplex) and on consumption C (e.g., box or wealth-proportional caps)—and highlight that *projection onto the PMP-optimal control manifold* scales to high-dimensional portfolios where DP grids are effectively impossible, naturally accommodates interacting policy constraints, and remains applicable when constrained closed-form policies are unknown or do not exist. Altogether, projecting onto the PMP-optimal control manifold enables scalable, constraint-respecting portfolio policies precisely in regimes where value-based grids are intractable and analytic solutions are unavailable.

The remainder of the paper is organized as follows. Section 2 briefly reviews the DP perspective and the classical Merton problem to set notation and highlight limitations under constraints. Section 3 presents the PMP formulation and the barrier-regularized projection onto the PMP-optimal control manifold. Section 4 describes the gradient-based training loop and its PMP correspondence. Section 5 reports constrained experiments: weight constraints in Section 5.1 and consumption constraints in Section 5.2, with quantitative comparisons (policy RMSE, Hamiltonian FOC residuals, and utility gaps). Section 6 concludes and outlines extensions.

2 Dynamic Programming Approach to Multi-Asset Portfolio Problems

This section reviews the multi-asset version of Merton’s portfolio problem (Merton, 1969, 1971) from a dynamic programming (DP) perspective. We first discuss the classical unconstrained setting, in which an investor continuously selects portfolio and consumption strategies. Although standard DP methods can, in theory, handle constraints through shadow prices or dual methods, practical constraints often prevent obtaining analytic solutions. This limitation motivates the Pontryagin-based approach developed in subsequent sections

2.1 DP Formulation and Unconstrained Merton Solution

We consider an investor who allocates wealth across $n + 1$ assets: a risk-free asset (indexed by $i = 0$) with drift r_t and zero volatility, and n risky assets (indices $i = 1, \dots, n$) with drifts $\mu_{i,t}$ and covariance Σ_t . In vector form, we define

$$\tilde{\boldsymbol{\mu}}_t = (r_t, \mu_{1,t}, \dots, \mu_{n,t})^\top, \quad \tilde{V}_t = \begin{bmatrix} \mathbf{0}_{1 \times n} \\ V_t \end{bmatrix},$$

so that $\Sigma_t = V_t V_t^\top$, and the first row of \tilde{V}_t is zero, reflecting the zero volatility of the risk-free asset.

Let X_t be the investor's wealth at time t , and let $\boldsymbol{\pi}_t = (\pi_{0,t}, \pi_{1,t}, \dots, \pi_{n,t})^\top$ denote the fraction of wealth invested in each asset, satisfying $\sum_{i=0}^n \pi_{i,t} = 1$. Without constraints on short-selling or borrowing, the wealth evolves as

$$dX_t = (X_t \boldsymbol{\pi}_t^\top \tilde{\boldsymbol{\mu}}_t - C_t) dt + X_t \boldsymbol{\pi}_t^\top \tilde{V}_t d\mathbf{W}_t, \quad X_0 = x_0 > 0,$$

where $C_t \geq 0$ represents the consumption rate.

The investor aims to maximize the expected discounted utility

$$J(\boldsymbol{\pi}, C) = \mathbb{E} \left[\int_0^T e^{-\rho t} U(C_t) dt + K e^{-\rho T} U(X_T) \right],$$

with an increasing and concave utility function U , discount rate $\rho > 0$, and bequest parameter $K \geq 0$.

To characterize optimal decisions, we define the value function $V(t, x)$ as the maximum achievable expected utility when starting from time t with wealth x :

$$V(t, x) = \max_{\boldsymbol{\pi}, C \geq 0} \mathbb{E} \left[\int_t^T e^{-\rho s} U(C_s) ds + K e^{-\rho T} U(X_T) \mid X_t = x \right]. \quad (1)$$

By dynamic programming, V satisfies the Hamilton–Jacobi–Bellman (HJB) equation

$$0 = \max_{\boldsymbol{\pi}, C \geq 0} \left\{ e^{-\rho t} U(C) + V_t + \left[x \boldsymbol{\pi}^\top \tilde{\boldsymbol{\mu}}_t - C \right] V_x + \frac{1}{2} x^2 (\boldsymbol{\pi}^\top \tilde{V}_t \tilde{V}_t^\top \boldsymbol{\pi}) V_{xx} \right\},$$

where subscripts V_t , V_x , V_{xx} denote partial derivatives. Note that the functional $J(\boldsymbol{\pi}, C)$ measures the expected utility under a given policy $(\boldsymbol{\pi}, C)$, while $V(t, x)$ represents the maximum achievable utility from each initial state (t, x) .

In the unconstrained case, one can derive first-order conditions (FOCs) by differentiating the HJB equation with respect to C and $\boldsymbol{\pi}$. The resulting pointwise-optimal controls $(\boldsymbol{\pi}_t^*, C_t^*)$ satisfy

$$\begin{aligned} \frac{\partial}{\partial C} \left[e^{-\rho t} U(C) - C V_x \right] &= 0 \implies e^{-\rho t} U'(C_t^*) = V_x(t, x), \\ \frac{\partial}{\partial \boldsymbol{\pi}} \left[x \boldsymbol{\pi}^\top \tilde{\boldsymbol{\mu}}_t V_x + \frac{1}{2} x^2 (\boldsymbol{\pi}^\top \tilde{V}_t \tilde{V}_t^\top \boldsymbol{\pi}) V_{xx} \right] &= \mathbf{0}. \end{aligned}$$

From the first equation, the optimal consumption takes the form

$$C_t^* = (U')^{-1} (e^{\rho t} V_x(t, x)),$$

so C_t^* depends on the inverse derivative of U and the marginal value of wealth V_x . Similarly, the second equation yields

$$\boldsymbol{\pi}_{1:n,t}^* = -\frac{x V_x(t, x)}{V_{xx}(t, x)} \Sigma_t^{-1} (\boldsymbol{\mu}_t - r_t \mathbf{1}),$$

providing an expression for the optimal portfolio in terms of V_x and V_{xx} . These expressions illustrate how optimal policies $(\boldsymbol{\pi}_t^*, C_t^*)$ can be analytically characterized in the unconstrained scenario.

However, analytic solutions are typically difficult to obtain under realistic constraints or general utility functions. We thus turn next to how such constraints affect the DP formulation and typically require numerical or alternative approaches.

2.2 Shadow-Price Formulation of Portfolio Constraints

A unifying viewpoint is that portfolio-consumption constraints can be represented through *shadow prices* (Lagrange multipliers) attached to admissibility conditions (e.g., Karatzas & Shreve, 1998; Fleming & Soner, 2006). Let the feasible set be described by inequalities

$$\Gamma_j(\boldsymbol{\pi}_t, C_t) \geq 0, \quad j = 1, \dots, m,$$

and consider the augmented Hamiltonian

$$\tilde{\mathcal{H}}(t, x, \boldsymbol{\pi}_t, C_t, \lambda_t, Z_t; \nu_t) = \mathcal{H}(t, x, \boldsymbol{\pi}_t, C_t, \lambda_t, Z_t) + \sum_{j=1}^m \nu_{j,t} \Gamma_j(\boldsymbol{\pi}_t, C_t), \quad \nu_{j,t} \geq 0.$$

The multipliers $\nu_{j,t}$ are the shadow prices: they quantify the marginal value of relaxing each constraint. Optimality imposes complementary slackness

$$\nu_{j,t} \Gamma_j(\boldsymbol{\pi}_t, C_t) = 0 \quad \text{for all } j, t,$$

so inactive constraints have zero shadow prices, while binding constraints carry strictly positive shadow prices. The main practical issue is not existence (ensured under convexity/KKT regularity) but *computability*: in a few canonical cases the multipliers are identified explicitly and yield (piecewise) closed-form policies; in general, finding the multipliers already amounts to solving a high-dimensional nonlinear free-boundary problem (Shreve & Soner, 1994; Fleming & Soner, 2006).

We now summarize several standard constraints in this shadow-price language.

- **Borrowing (no leverage).** The nonnegativity of the money-market position $\pi_{0,t} \geq 0$ can be encoded by a *shadow rate* $r^* \geq r$ that raises the effective borrowing cost when the constraint binds. In the single-asset CRRA case, r^* admits an explicit expression, so replacing r by r^* in the unconstrained Merton formulas yields closed-form consumption/portfolio rules (see Karatzas & Shreve, 1998).
- **Short sales (risky assets).** For $\pi_{i,t} \geq 0$ ($i = 1, \dots, n$), introduce multipliers $\nu_{i,t} \geq 0$ with $\nu_{i,t} \pi_{i,t} = 0$. In CRRA with constant (μ, Σ) , fixing an active set \mathcal{A} (indices with $\pi_i > 0$) and writing $\alpha = \mu - r\mathbf{1}$, the KKT system with full-investment shadow price $\eta \geq 0$ yields the *piecewise closed form*

$$\pi_{\mathcal{A}} = \frac{1}{\gamma} \Sigma_{\mathcal{A}\mathcal{A}}^{-1} (\alpha_{\mathcal{A}} - \eta \mathbf{1}_{\mathcal{A}}), \quad \pi_{\mathcal{A}^c} = 0,$$

with either $\mathbf{1}_{\mathcal{A}}^\top \pi_{\mathcal{A}} < 1$ (thus $\eta = 0$) or, if $\mathbf{1}_{\mathcal{A}}^\top \pi_{\mathcal{A}} = 1$,

$$\eta = \frac{\mathbf{1}_{\mathcal{A}}^\top \Sigma_{\mathcal{A}\mathcal{A}}^{-1} \alpha_{\mathcal{A}} - \gamma}{\mathbf{1}_{\mathcal{A}}^\top \Sigma_{\mathcal{A}\mathcal{A}}^{-1} \mathbf{1}_{\mathcal{A}}}.$$

See, e.g., Karatzas et al. (1987) and Cvitanić & Karatzas (1996) for KKT/shadow-price treatments of portfolio constraints.

- **Consumption bounds (box constraints).** For

$$C_{\min} \leq C_t \leq C_{\max}, \quad (2)$$

include *consumption shadow prices* $\alpha_t, \beta_t \geq 0$ in $\tilde{\mathcal{H}} = \mathcal{H} + \alpha_t(C_t - C_{\min}) + \beta_t(C_{\max} - C_t)$. The FOC and slackness

$$e^{-\rho t} U'(C_t) - \lambda_t + \alpha_t - \beta_t = 0, \quad \alpha_t(C_t - C_{\min}) = 0, \quad \beta_t(C_{\max} - C_t) = 0$$

imply the closed-form policy

$$C_t^* = \min \left\{ \max \{ (U')^{-1}(e^{\rho t} \lambda_t), C_{\min} \}, C_{\max} \right\},$$

cf. standard HJB/PMP derivations in Fleming & Soner (2006).

- **Consumption ratcheting (path dependence).** For $C_t \geq \max_{s < t} C_s$, augment the state by $Y_t = \max_{s \leq t} C_s$ and attach a multiplier $\zeta_t \geq 0$ to $C_t - Y_t \geq 0$. The formulation remains valid but lifts the value function to $V(t, x, y)$ on an enlarged state; the induced free-boundary problem admits no general closed form and is typically solved numerically (duality/optimal stopping or FBSDE), except in narrow cases; see Dybvig (1995) for ratcheting and Constantinides (1990); Sundaresan (1989) for related habit-formation models.

In summary, shadow prices provide a single, coherent language for constraints. For borrowing, short selling, and box consumption, multipliers are often identified quickly and yield closed-form or piecewise closed-form policies. For path-dependent restrictions and interacting linear constraints (e.g., sector caps), computing the multipliers becomes the main obstacle—effectively a high-dimensional free-boundary problem. This motivates the Pontryagin-based method developed next, which enforces feasibility via projections or barriers without explicitly solving for shadow prices in high dimension.

3 Pontryagin's Maximum Principle Approach to Multi-Asset Portfolio Optimization

This section presents PMP as an alternative framework to the DP methods discussed in Section 2. We show first how PMP recovers the classical Merton solution in an unconstrained setting, and then extend the analysis to scenarios with practical constraints, where projection or barrier methods can be used to handle complex investment or consumption restrictions without resorting to high-dimensional PDEs.

3.1 Unconstrained Case: Formulation and Optimal Solutions

We first consider the multi-asset Merton problem without borrowing, short-selling, or explicit consumption constraints, as discussed previously in Section 2.1. Under PMP, originally introduced by Pontryagin (2018) and extensively discussed in subsequent works such as Pardoux & Peng (1990), Fleming & Soner (2006), and Pham (2009), one derives a system of forward-backward stochastic differential equations (FBSDEs) characterizing optimal solutions. Central to this approach is the introduction of adjoint processes, consisting of a scalar adjoint λ_t associated with the state variable X_t and a vector adjoint $\mathbf{Z}_t \in \mathbb{R}^n$ linked to the n -dimensional Brownian motion \mathbf{W}_t driving asset returns.

To apply the PMP to our setting, we introduce the Hamiltonian defined by

$$\mathcal{H}(t, X_t, \boldsymbol{\pi}_t, C_t, \lambda_t, \mathbf{Z}_t) = e^{-\rho t} U(C_t) + \lambda_t \left[X_t \boldsymbol{\pi}_t^\top \tilde{\mu}_t - C_t \right] + \mathbf{Z}_t^\top \left(X_t \tilde{V}_t^\top \boldsymbol{\pi}_t \right), \quad (3)$$

where the adjoint $\lambda_t \approx \partial J / \partial X_t$ can be interpreted economically as the marginal value of an incremental unit of wealth at time t , and \mathbf{Z}_t measures the sensitivity of the adjoint with respect to stochastic fluctuations in asset prices.

Under optimal controls $(\boldsymbol{\pi}_t^*, C_t^*)$, the state and adjoint processes must satisfy the following coupled FBSDE system:

$$dX_t^* = \left[X_t^* (\boldsymbol{\pi}_t^*)^\top \tilde{\mu}_t - C_t^* \right] dt + X_t^* (\boldsymbol{\pi}_t^*)^\top \tilde{V}_t d\mathbf{W}_t, \quad X_0^* = x_0, \quad (4)$$

$$d\lambda_t^* = - \frac{\partial \mathcal{H}}{\partial X} (t, X_t^*, \boldsymbol{\pi}_t^*, C_t^*, \lambda_t^*, \mathbf{Z}_t^*) dt + \mathbf{Z}_t^{*\top} d\mathbf{W}_t, \quad \lambda_T^* = K e^{-\rho T} U'(X_T^*). \quad (5)$$

Maximization of the Hamiltonian at each instant yields the first-order optimality conditions with respect to consumption and portfolio weights:

$$\frac{\partial \mathcal{H}}{\partial C_t} = e^{-\rho t} U'(C_t^*) - \lambda_t^* = 0, \quad (6)$$

which indicates that optimal consumption equates marginal discounted utility to the marginal adjoint value. Thus, the optimal consumption can be expressed as

$$C_t^* = (U')^{-1} (e^{\rho t} \lambda_t^*). \quad (7)$$

Similarly, the optimal portfolio allocation satisfies the first-order condition obtained from differentiating the Hamiltonian (3) with respect to the portfolio weights $\boldsymbol{\pi}_t$:

$$\frac{\partial \mathcal{H}}{\partial \boldsymbol{\pi}_t} = \lambda_t^* X_t^* \tilde{\mu}_t + X_t^* \tilde{V}_t^\top \mathbf{Z}_t^* = \mathbf{0}. \quad (8)$$

Solving explicitly for the risky-asset weights gives

$$\boldsymbol{\pi}_{1:n,t}^* = - \frac{\lambda_t^*}{X_t^* (\partial_x \lambda_t^*)} \Sigma_t^{-1} (\boldsymbol{\mu}_t - r_t \mathbf{1}), \quad (9)$$

thus recovering the classical Merton solution structure within the multi-asset context.

This PMP formulation transforms the optimization problem into a more tractable system of FBSDEs. Unlike standard DP approaches that require discretization of high-dimensional PDEs, the FBSDE representation utilizes modern computational techniques, such as automatic differentiation and neural network approximations, thus significantly enhancing the scalability and practical applicability of the approach.

3.2 Constrained Case: KKT vs. Barrier

As discussed in §2.2, portfolio-consumption constraints (no borrowing/shorting, box consumption, sector caps, ratcheting, and related policies) admit a unified shadow-price formulation (e.g., Shreve & Soner, 1994; Fleming & Soner, 2006). Within the Pontryagin framework, one maximizes an augmented Hamiltonian that either carries explicit Lagrange multipliers (KKT view) or a logarithmic interior-point barrier (barrier view) (Nesterov & Nemirovskii, 1994; Boyd, 2004; Wright, 1997). The two formulations are equivalent in the limit $\epsilon \downarrow 0$; they differ mainly in numerical handling, with the barrier following the central path.

In the KKT view, let $\Gamma_j(\boldsymbol{\pi}_t, C_t) \geq 0$ for $j = 1, \dots, m$ encode the inequality constraints and impose full investment $\sum_{i=0}^n \pi_{i,t} = 1$. With multipliers $\nu_{j,t} \geq 0$ and $\eta_t \in \mathbb{R}$, define

$$\tilde{\mathcal{H}}_{\text{KKT}} = \mathcal{H} + \eta_t \left(1 - \sum_{i=0}^n \pi_{i,t} \right) + \sum_{j=1}^m \nu_{j,t} \Gamma_j(\boldsymbol{\pi}_t, C_t). \quad (10)$$

Stationarity with respect to (π, C) , primal feasibility, dual feasibility, and complementary slackness $\nu_{j,t}\Gamma_j(\pi_t, C_t) = 0$ characterize constrained maximizers (Bertsekas, 1997). Shadow prices are zero when a constraint is inactive and strictly positive when it binds.

In the barrier view, explicit multipliers are replaced by a log barrier that keeps the iterate in the strict interior:

$$\tilde{\mathcal{H}}_{\text{bar}} = \mathcal{H} + \eta_t \left(1 - \sum_{i=0}^n \pi_{i,t} \right) - \epsilon \sum_{j=1}^m \ln(\Gamma_j(\pi_t, C_t)), \quad \epsilon > 0. \quad (11)$$

First-order conditions for (11) converge to those of (10) as $\epsilon \downarrow 0$, with the central-path identification $\nu_{j,t} = \epsilon/\Gamma_j(\pi_t, C_t)$ (Nesterov & Nemirovskii, 1994; Wright, 1997). This connection underlies the policy and Hamiltonian gap bounds in §3.3.

At a fixed time-state (t, x) , stagewise maximization of (11) leads to the system

$$\mathbf{F}(\pi, \eta) = \begin{pmatrix} \nabla_\pi \tilde{\mathcal{H}}_{\text{bar}}(t, x; \pi, C, \eta) \\ \mathbf{1}^\top \pi - 1 \end{pmatrix} = \mathbf{0},$$

which is solved in the tangent space $\{\mathbf{1}^\top d = 0\}$ by a Newton step that requires only Hessian-vector products (Newton-CG) (Nocedal & Wright, 2006). Writing $g := \nabla_\pi \tilde{\mathcal{H}}_{\text{bar}}$ and denoting by $H_{\text{bar}}[\cdot]$ the reduced Hessian operator, the search direction d satisfies $H_{\text{bar}}[d] = -g + \eta \mathbf{1}$ in the subspace. For general constraints one obtains

$$H_{\text{bar}}[v] = \nabla_{\pi\pi}^2 \mathcal{H} v + \epsilon \sum_{l=1}^m \frac{1}{\Gamma_l(\pi, C)^2} \left(\nabla_\pi \Gamma_l \nabla_\pi \Gamma_l^\top v \right) - \epsilon \sum_{l=1}^m \frac{1}{\Gamma_l(\pi, C)} \nabla_{\pi\pi}^2 \Gamma_l v, \quad (12)$$

while for pure nonnegativity $\Gamma_i(\pi, C) = \pi_i$ it simplifies to

$$H_{\text{bar}}[v] = \nabla_{\pi\pi}^2 \mathcal{H} v + \text{diag}(\epsilon/\pi^2) v, \quad (13)$$

that is, the Hamiltonian Hessian plus a diagonal barrier term that improves conditioning (Boyd, 2004). The full-investment equality is handled either by orthogonal projection onto $\{\mathbf{1}^\top d = 0\}$ or via a 1×1 Schur complement in η (Nocedal & Wright, 2006).

Globalization and feasibility are enforced by a fraction-to-the-boundary line search with an Armijo condition (Wright, 1997; Wächter & Biegler, 2006). Starting from the maximal step that maintains strict interior feasibility,

$$\alpha_{\text{max}} = \min \left\{ 1, \min_{i: d_i < 0} [-\tau \pi_i / d_i] \right\}, \quad \tau \in (0, 1),$$

(or, for general Γ_j , by requiring $\Gamma_j(\pi + \alpha d, C + \alpha s) \geq (1 - \tau) \Gamma_j(\pi, C)$ for all j), one backtracks until the Armijo increase condition holds for maximization. This guarantees monotone ascent while staying strictly inside the feasible region (Wright, 1997; Boyd, 2004). The consumption block is scalar. With box constraints, one may use the closed form

$$C^* = \min \left\{ \max \{ (U')^{-1}(e^{\rho t} \lambda_t), C_{\text{min}} \}, C_{\text{max}} \right\},$$

and, under a barrier, the stationarity condition

$$e^{-\rho t} U'(C) - \lambda_t + \frac{\epsilon}{C - C_{\text{min}}} - \frac{\epsilon}{C_{\text{max}} - C} = 0$$

is solved by a short damped Newton step with the same line-search logic (Nocedal & Wright, 2006; Boyd, 2004).

Strong concavity of the Hamiltonian along feasible directions and LICQ at the active set yield a nonsingular KKT matrix and thus local quadratic (Newton) or fast superlinear (Newton-CG) convergence on the interior (Bertsekas, 1997; Nocedal & Wright, 2006). In practice, only a few inner iterations and a single backtracking loop suffice to reduce the stagewise residual to the tolerance needed by the outer learning loop; there is no need to oversolve the microproblem. The resulting barrier maximizers trace the central path and, by Theorem 1.

3.3 Barrier Policy Error Bounds

We provide rigorous error bounds that compare the policy obtained by maximizing the barrier-augmented Hamiltonian with the true constrained PMP/KKT policy at a fixed time-state. Throughout this subsection we suppress explicit dependence on (t, x) and adjoints (λ_t, Z_t) for readability.

Assumption 1 (Regularity and geometry). *Let $\mathcal{H}(\pi, C)$ be twice continuously differentiable on a neighborhood of the constrained maximizer (π^*, C^*) .*

(i) (Strong concavity along feasible directions) *Let $h(\pi) = \mathbf{1}^\top \pi - 1 = 0$ be the full-investment equality. There exists $\mu > 0$ such that for all feasible directions d with $\mathbf{1}^\top d = 0$,*

$$-d^\top \nabla_{\pi\pi}^2 \mathcal{H}(\pi^*, C^*) d \geq \mu \|d\|^2.$$

(ii) (Smooth constraints and LICQ) *Inequalities $\Gamma_j(\pi, C) \geq 0$ ($j = 1, \dots, m$) are C^2 and at (π^*, C^*) the gradients $\{\nabla_\pi \Gamma_j\}_{j \in \mathcal{A}} \cup \{\mathbf{1}\}$ are linearly independent, where \mathcal{A} is the active set $\{j : \Gamma_j(\pi^*, C^*) = 0\}$.*

(iii) (Strict complementarity) *There exist KKT multipliers (ν^*, η^*) with $\nu_j^* > 0$ for $j \in \mathcal{A}$ and $\nu_j^* = 0$ for $j \notin \mathcal{A}$.*

(iv) (Smoothness) *$\nabla_\pi \mathcal{H}$ is L -Lipschitz in π on a neighborhood of π^* .*

(v) (State and reward Lipschitzness) *The wealth SDE coefficients are Lipschitz in (π, C) and the marginal utility is locally Lipschitz on the relevant compact set.*

Remark 1 (Sign convention). *For rigorous alignment with interior-point calculus, it is convenient to recast inequalities as $g_j(\pi, C) \leq 0$ with $g_j := -\Gamma_j$. The KKT Lagrangian then reads $\mathcal{L} = \mathcal{H} + \eta h + \sum_j \nu_j g_j$ with $\nu_j \geq 0$, and the log-barrier is $-\epsilon \sum_j \ln(-g_j) = -\epsilon \sum_j \ln \Gamma_j$. This yields the same stationarity signs as used below. For notational continuity with §2.2, we continue to write $\Gamma_j \geq 0$, bearing in mind that derivatives appear with the appropriate sign.*

We first relate the barrier first-order conditions to a perturbed KKT system.

Lemma 1 (Barrier stationarity as perturbed KKT). *Let $(\hat{\pi}_\epsilon, \hat{C}_\epsilon, \hat{\eta}_\epsilon)$ maximize the barrier Hamiltonian*

$$\tilde{\mathcal{H}}_{\text{bar}} = \mathcal{H}(\pi, C) + \eta(1 - \mathbf{1}^\top \pi) - \epsilon \sum_{j=1}^m \ln \Gamma_j(\pi, C), \quad \epsilon > 0,$$

on the strictly feasible region $\{\Gamma_j > 0\}$. Define

$$\hat{\nu}_{j,\epsilon} := \frac{\epsilon}{\Gamma_j(\hat{\pi}_\epsilon, \hat{C}_\epsilon)}, \quad j = 1, \dots, m.$$

Then $(\hat{\pi}_\epsilon, \hat{C}_\epsilon, \hat{\eta}_\epsilon, \hat{\nu}_\epsilon)$ satisfies

$$\nabla_\pi \mathcal{H}(\hat{\pi}_\epsilon, \hat{C}_\epsilon) - \hat{\eta}_\epsilon \mathbf{1} - \sum_{j=1}^m \hat{\nu}_{j,\epsilon} \nabla_\pi \Gamma_j(\hat{\pi}_\epsilon, \hat{C}_\epsilon) = 0, \quad (14)$$

$$\mathbf{1}^\top \hat{\pi}_\epsilon = 1, \quad (15)$$

$$\hat{\nu}_{j,\epsilon} \Gamma_j(\hat{\pi}_\epsilon, \hat{C}_\epsilon) = \epsilon, \quad \hat{\nu}_{j,\epsilon} > 0, \quad \Gamma_j(\hat{\pi}_\epsilon, \hat{C}_\epsilon) > 0. \quad (16)$$

Proof. Differentiating $\tilde{\mathcal{H}}_{\text{bar}}$ in π and C and setting the derivatives to zero gives (14) with $\hat{\nu}_{j,\epsilon} = \epsilon / \Gamma_j$, while differentiation in η yields the equality constraint (15). By construction, (16) holds and strict feasibility follows from the barrier domain. \square

We now show that the barrier solution approaches the KKT solution at first order in ϵ .

Lemma 2 (Linearization around the KKT point). *Under Assumption 1, define the active set \mathcal{A} at (π^*, C^*) . Then for ϵ sufficiently small, there exists a unique strictly feasible $(\hat{\pi}_\epsilon, \hat{C}_\epsilon, \hat{\eta}_\epsilon, \hat{\nu}_\epsilon)$ solving (14)–(16) in a neighborhood of $(\pi^*, C^*, \eta^*, \nu^*)$ with $\hat{\nu}_{j,\epsilon} \rightarrow \nu_j^*$ for $j \in \mathcal{A}$ and $\hat{\nu}_{j,\epsilon} = O(\epsilon)$ for $j \notin \mathcal{A}$. Moreover,*

$$\|\hat{\pi}_\epsilon - \pi^*\| + |\hat{\eta}_\epsilon - \eta^*| + \sum_{j \in \mathcal{A}} |\hat{\nu}_{j,\epsilon} - \nu_j^*| \leq c\epsilon$$

for some constant $c > 0$ independent of ϵ .

Proof. Consider the mapping

$$G(\pi, \eta, \nu; \epsilon) = \begin{pmatrix} \nabla_\pi \mathcal{H}(\pi, C^*) - \eta \mathbf{1} - \sum_{j=1}^m \nu_j \nabla_\pi \Gamma_j(\pi, C^*) \\ \mathbf{1}^\top \pi - 1 \\ (\nu_j \Gamma_j(\pi, C^*) - \epsilon)_{j \in \mathcal{A}} \\ (\nu_j)_{j \notin \mathcal{A}} \end{pmatrix}.$$

At $(\pi^*, \eta^*, \nu^*; 0)$ we have $G = 0$ by KKT with strict complementarity. Its Jacobian with respect to $(\pi, \eta, \nu_{\mathcal{A}})$ at $\epsilon = 0$ is the standard KKT matrix restricted to the active set,

$$\mathcal{K} = \begin{pmatrix} \nabla_{\pi\pi}^2 \mathcal{L}^* & -\mathbf{1} & -[\nabla_\pi \Gamma_{\mathcal{A}}] \\ -\mathbf{1}^\top & 0 & 0 \\ [\nabla_\pi \Gamma_{\mathcal{A}}]^\top & 0 & \text{diag}(\Gamma_{\mathcal{A}}^*) \end{pmatrix} = \begin{pmatrix} \nabla_{\pi\pi}^2 \mathcal{L}^* & -\mathbf{1} & -[\nabla_\pi \Gamma_{\mathcal{A}}] \\ -\mathbf{1}^\top & 0 & 0 \\ [\nabla_\pi \Gamma_{\mathcal{A}}]^\top & 0 & 0 \end{pmatrix},$$

where $\mathcal{L}^*(\pi) = \mathcal{H}(\pi, C^*) - \eta^* \mathbf{1}^\top \pi - \sum_{j \in \mathcal{A}} \nu_j^* \Gamma_j(\pi, C^*)$ and the last block uses $\Gamma_{\mathcal{A}}^* = 0$. LICQ and strong second-order sufficiency (item (i)) imply that \mathcal{K} is nonsingular on the tangent space $\{\mathbf{1}^\top d = 0, \nabla_\pi \Gamma_{\mathcal{A}}^\top d = 0\}$ (standard KKT regularity). Augmenting G with the inactive dual feasibility rows $\nu_j = 0$ for $j \notin \mathcal{A}$ makes the full Jacobian nonsingular (strict complementarity). By the Implicit Function Theorem, there exists a unique C^1 curve $(\hat{\pi}_\epsilon, \hat{\eta}_\epsilon, \hat{\nu}_{\mathcal{A},\epsilon}, \epsilon)$ with $G(\hat{\pi}_\epsilon, \hat{\eta}_\epsilon, \hat{\nu}_\epsilon, \epsilon) = 0$ and

$$\begin{pmatrix} \hat{\pi}_\epsilon - \pi^* \\ \hat{\eta}_\epsilon - \eta^* \\ \hat{\nu}_{\mathcal{A},\epsilon} - \nu_{\mathcal{A}}^* \end{pmatrix} = -\mathcal{K}^{-1} \begin{pmatrix} 0 \\ 0 \\ \epsilon \mathbf{1}_{|\mathcal{A}|} \end{pmatrix} + o(\epsilon),$$

whence the claimed $O(\epsilon)$ bounds. For $j \notin \mathcal{A}$ the last block enforces $\hat{\nu}_{j,\epsilon} = 0 + O(\epsilon)$, as written. \square

We can now state and prove the main result.

Theorem 1 (Barrier vs. KKT policy: first-order accuracy). *Under Assumption 1, there exist constants $K, \kappa_1, \kappa_2 > 0$ (independent of ϵ) and $\bar{\epsilon} > 0$ such that, for all $0 < \epsilon \leq \bar{\epsilon}$, the barrier maximizer $(\hat{\pi}_\epsilon, \hat{C}_\epsilon)$ satisfies*

$$\|\hat{\pi}_\epsilon - \pi^*\| \leq K\epsilon, \tag{17}$$

$$0 \leq \mathcal{H}(\pi^*, C^*) - \mathcal{H}(\hat{\pi}_\epsilon, \hat{C}_\epsilon) \leq \frac{LK^2}{2} \epsilon^2, \tag{18}$$

$$0 \leq J(\pi^*, C^*) - J(\hat{\pi}_\epsilon, \hat{C}_\epsilon) \leq \kappa_1 \epsilon^2 + \kappa_2 \epsilon. \tag{19}$$

Proof. By Lemma 2, $\Delta\pi_\epsilon := \hat{\pi}_\epsilon - \pi^* = O(\epsilon)$ and $\Delta\eta_\epsilon = \hat{\eta}_\epsilon - \eta^* = O(\epsilon)$, with $\hat{\nu}_{j,\epsilon} - \nu_j^* = O(\epsilon)$ for $j \in \mathcal{A}$ and $\hat{\nu}_{j,\epsilon} = O(\epsilon)$ for $j \notin \mathcal{A}$.

Subtract the stationarity equations at $(\hat{\pi}_\epsilon, \hat{C}_\epsilon)$ and (π^*, C^*) :

$$\nabla_\pi \mathcal{H}(\hat{\pi}_\epsilon, \hat{C}_\epsilon) - \nabla_\pi \mathcal{H}(\pi^*, C^*) - (\hat{\eta}_\epsilon - \eta^*) \mathbf{1} - \sum_{j=1}^m \left(\hat{\nu}_{j,\epsilon} \nabla_\pi \Gamma_j(\hat{\pi}_\epsilon, \hat{C}_\epsilon) - \nu_j^* \nabla_\pi \Gamma_j(\pi^*, C^*) \right) = 0.$$

Project onto the tangent space of $h(\pi) = 0$ using the orthogonal projector $P := I - \frac{1}{n+1} \mathbf{1} \mathbf{1}^\top$ so that $P\mathbf{1} = 0$ and $P\Delta\pi_\epsilon = \Delta\pi_\epsilon$. By the mean-value theorem and Lipschitzness,

$$\left\| P \left(\nabla_\pi \mathcal{H}(\hat{\pi}_\epsilon, \hat{C}_\epsilon) - \nabla_\pi \mathcal{H}(\pi^*, C^*) \right) \right\| \geq \mu \|\Delta\pi_\epsilon\|,$$

where we used strong concavity along feasible directions (Assumption 1(i)). The remaining projected term is bounded by

$$\left\| P \sum_{j=1}^m \left(\hat{\nu}_{j,\epsilon} \nabla_\pi \Gamma_j(\hat{\pi}_\epsilon, \hat{C}_\epsilon) - \nu_j^* \nabla_\pi \Gamma_j(\pi^*, C^*) \right) \right\| \leq c_1 \epsilon,$$

because $\hat{\nu}_{j,\epsilon} - \nu_j^* = O(\epsilon)$ and $\nabla_\pi \Gamma_j(\hat{\pi}_\epsilon, \hat{C}_\epsilon) - \nabla_\pi \Gamma_j(\pi^*, C^*) = O(\epsilon)$ by smoothness and Lemma 2. Hence $\mu \|\Delta\pi_\epsilon\| \leq c_1 \epsilon$, proving (17) with $K = c_1/\mu$.

For the Hamiltonian gap, L -smoothness gives

$$\mathcal{H}(\pi^*, C^*) - \mathcal{H}(\hat{\pi}_\epsilon, \hat{C}_\epsilon) \leq \frac{L}{2} \|\Delta\pi_\epsilon\|^2 \leq \frac{LK^2}{2} \epsilon^2,$$

which is (18). Finally, let X^* and \hat{X}_ϵ be the wealth processes under (π^*, C^*) and $(\hat{\pi}_\epsilon, \hat{C}_\epsilon)$. The drift/diffusion Lipschitz property and Grönwall's lemma imply

$$\sup_{s \in [t, T]} \mathbb{E} |X_s^* - \hat{X}_{\epsilon,s}| \leq c_2 \int_t^T \mathbb{E} (\|\Delta\pi_\epsilon\| + |\hat{C}_\epsilon - C^*|) ds \leq c_3 ((T-t) K \epsilon + \|\hat{C}_\epsilon - C^*\|_{L^1}).$$

The consumption block is handled exactly as for π (either box constraints, where the barrier and KKT truncations coincide up to numerical tolerance, or by the same argument), hence $\|\hat{C}_\epsilon - C^*\|_{L^1} = O(\epsilon)$. Local Lipschitzness of marginal utility yields (19) with suitable constants κ_1, κ_2 . \square

Remark 2 (Explicit modulus for Merton). *In the CRRA multi-asset Merton model, $\nabla_{\pi\pi}^2 \mathcal{H}(\pi, C) = -X_t^2 (\partial_x \lambda_t) \Sigma$ on risky coordinates. If $-\partial_x \lambda_t \geq \underline{\ell} > 0$ and $\lambda_{\min}(\Sigma) \geq \underline{\sigma} > 0$ on the training domain while $X_t \in [X_{\min}, X_{\max}]$, then Assumption 1(i) holds with $\mu \geq X_{\min}^2 \underline{\ell} \underline{\sigma}$, so the constant K in (17) can be made fully explicit.*

4 Gradient-Based Algorithm for Policy Optimization

This section extends the unconstrained gradient-PMP algorithm of Huh et al. (2025) to fully *constrained* portfolio-consumption settings. All inequalities are enforced by a log-barrier microproblem solved at each time-state, so the stagewise update remains on (an approximation of) the Pontryagin/KKT manifold. The rollout (exponential-Euler) and BPTT adjoints are unchanged; the only additions are: (i) replacing the unconstrained stagewise update with the barrier-augmented one, and (ii) an optional *manifold-projection* variant (P-PGDPO) that uses stabilized adjoints to project the control onto the barrier-augmented Hamiltonian.

4.1 Extended Objective with Barrier Enforcement

Let ν be a sampling distribution over a training domain $\mathcal{D} \subset [0, T) \times (0, \infty) \times \mathbb{R}^k$ of initial time-wealth-state triplets (t_0, x_0, y_0) . The extended objective reads

$$J_e(\theta, \phi) = \mathbb{E}_{(t_0, x_0, y_0) \sim \nu} \left[\mathbb{E} \left(\int_{t_0}^T e^{-\rho(u-t_0)} U(C_\phi(u, X_u, Y_u)) du + \kappa e^{-\rho(T-t_0)} U(X_T) \right) \right]. \quad (20)$$

Feasibility is not handled by output projections or shadow prices: *at every* time-state (t, x, y) we determine the controls (π, C) by maximizing the *barrier-augmented Hamiltonian* (see §3.2)

$$\tilde{\mathcal{H}}_{\text{bar}} = \mathcal{H} + \eta \left(1 - \sum_{i=0}^n \pi_i \right) - \epsilon \sum_{j=1}^m \ln \Gamma_j(\pi, C), \quad \epsilon > 0, \quad (21)$$

where $\Gamma_j(\pi, C) > 0$ encode all inequality constraints (e.g., nonnegativity of weights or box constraints on C) and η enforces full investment. Choosing a small ϵ controls the accuracy-cost tradeoff; §3.3 provides $O(\epsilon)$ policy error and $O(\epsilon^2)$ instantaneous Hamiltonian gap bounds.

4.2 Baseline PG-DPO (Activation-Constrained Gradients)

We train the policy by plain backpropagation-through-time (BPTT) while enforcing feasibility directly at the network outputs via smooth activations that map unconstrained logits to the feasible set. This keeps the entire rollout graph differentiable end-to-end and removes the need to solve a microproblem at every step. The activation layer supports the same four constraint types introduced in §2.2: no borrowing, no short-sales, box constraints on consumption, and consumption ratcheting.

- **No borrowing and no short-sales (full-investment simplex).** When both constraints are present, we place *all* n risky assets plus cash ($i = 0$) on the simplex via a softmax:

$$\pi_i(t, x, y) = \frac{\exp(u_i(t, x, y)/\tau)}{\sum_{j=0}^n \exp(u_j(t, x, y)/\tau)}, \quad i = 0, \dots, n, \quad (22)$$

so that $\sum_{i=0}^n \pi_i = 1$, $\pi_i \geq 0$, and in particular $\pi_0 \geq 0$ enforces no borrowing while $\pi_{1:n} \geq 0$ enforces no short-sales.

- **Separated parameterization for borrowing vs. short-sales (optional).** If one wishes to mirror the separation in §2.2 (borrowing handled by cash, short-sales by risky weights), we parameterize risky weights on the simplex and scale them by a *budget share* $a \in (0, 1)$:

$$w_i(t, x, y) = \frac{\exp(\tilde{u}_i/\tau)}{\sum_{j=1}^n \exp(\tilde{u}_j/\tau)}, \quad a(t, x, y) = \sigma(\tilde{a}), \quad \pi_{1:n} = a w, \quad \pi_0 = 1 - a. \quad (23)$$

Then $\pi_{1:n} \geq 0$ imposes the short-sales ban and $\pi_0 \geq 0$ imposes the borrowing ban. If borrowing is allowed but short-sales are not, one may replace $a = \sigma(\tilde{a})$ by $a = \text{softplus}(\tilde{a})$ so that $\pi_0 = 1 - a$ can be negative while $\pi_{1:n} \geq 0$ is maintained.

- **Box-constrained consumption (including nonnegativity as a special case).** For $C_{\min} \leq C_t \leq C_{\max}$ with an unconstrained logit $v(t, x, y) \in \mathbb{R}$,

$$C(t, x, y) = \frac{C_{\max} + C_{\min}}{2} + \frac{C_{\max} - C_{\min}}{2} \tanh v(t, x, y). \quad (24)$$

The one-sided nonnegativity $C_t \geq 0$ corresponds to $C_{\min} = 0$; if desired, the simple map $C = \alpha \text{softplus}(v)$ with $\alpha > 0$ can also be used.

- **Consumption ratcheting.** For the path-dependent constraint $C_t \geq Y_t$ with $Y_t = \max_{s \leq t} C_s$, we augment the state by Y and map

$$C(t, x, y) = y + \text{softplus}(v(t, x, y)), \quad (25)$$

which enforces $C \geq Y$ by construction while preserving smoothness. In the rollout, Y is updated by $Y_{k+1} = \max\{Y_k, C_k\}$.

Given (π_k, C_k) from the activations above, we evolve wealth with the exponential–Euler scheme

$$X_{k+1} = X_k \exp\left(\left[\pi_k^\top \tilde{\mu}_k - \frac{1}{2} \pi_{1:n,k}^\top \Sigma_k \pi_{1:n,k} - C_k/X_k\right] \Delta t + \pi_k^\top \tilde{V}_k \Delta W_k\right). \quad (26)$$

We then apply BPTT with respect to (θ, ϕ) through (26) and the activation maps (22)–(25). The resulting pathwise adjoints $(\lambda_k, \mathbf{Z}_k)$ yield the practical gradient estimators

$$\nabla_\theta J_e \approx \mathbb{E} \left[\sum_k \left\{ \lambda_k X_k \tilde{\mu}_k + X_k (\tilde{V}_k \mathbf{Z}_k) \right\}^\top \frac{\partial \pi_\theta(t_k, X_k, Y_k)}{\partial \theta} \Delta t \right], \quad (27)$$

$$\nabla_\phi J_e \approx \mathbb{E} \left[\sum_k \left(-\lambda_k + e^{-\rho t_k} U'(C_k) \right) \frac{\partial C_\phi(t_k, X_k, Y_k)}{\partial \phi} \Delta t \right]. \quad (28)$$

The following theoretical link clarifies when autodiff adjoints are the “right” objects from optimal control. In continuous-time stochastic control, the correct sensitivities are the Pontryagin costates solving the backward (S)DE coupled to the forward dynamics. If BPTT adjoints did not align with these costates—e.g., by propagating through constraint maps or nonstationary stagewise controls—then policy gradients could drift from PMP first-order conditions, harming both sample efficiency and structural fidelity. We therefore formalize the conditions under which the BPTT recursion *matches or approximates* the constrained PMP costate dynamics. This result extends the unconstrained correspondence in Huh et al. (2025, Thm. 3) to activation/barrier-constrained policies by replacing the plain Hamiltonian with its barrier-augmented counterpart and accounting for ε_k -stationarity.

Theorem 2 (Approximate BPTT–PMP correspondence under activation or barrier constraints). *Assume the regularity and feasibility conditions in Assumption 2. At time step k , let (π_k, C_k, η_k) be either (i) the exact maximizer of the barrier-augmented Hamiltonian $\tilde{\mathcal{H}}_{\text{bar}}(t_k, X_k, Y_k; \pi, C, \eta, \lambda_{k+1}, Z_{k+1})$, or (ii) an ε_k -stationary point produced by smooth activations, i.e., $\|\nabla_{\pi, C} \tilde{\mathcal{H}}_{\text{bar}}\| \leq \varepsilon_k$. Then the BPTT adjoint recursion satisfies*

$$\lambda_k - \lambda_{k+1} = \Delta t \partial_x \tilde{\mathcal{H}}_{\text{bar}}(t_k, X_k, Y_k; \pi_k, C_k, \eta_k, \lambda_{k+1}, Z_{k+1}) - Z_{k+1}^\top \Delta W_k + r_k,$$

with conditional mean error $\mathbb{E}[r_k | \mathcal{F}_{t_k}] = O(\Delta t^{3/2} + \varepsilon_k \Delta t)$. Consequently,

$$\mathbb{E}[\lambda_k - \lambda_{k+1} | \mathcal{F}_{t_k}] = \Delta t \partial_x \tilde{\mathcal{H}}_{\text{bar}}(t_k, X_k, Y_k; \pi_k, C_k, \eta_k, \lambda_{k+1}, Z_{k+1}) + O(\Delta t^{3/2} + \varepsilon_k \Delta t).$$

In particular: (a) if the barrier microproblem is solved exactly ($\varepsilon_k = 0$), the BPTT recursion matches the constrained PMP costate dynamics up to the standard time-discretization error; (b) under activation-only feasibility, the estimator exhibits an $O(\varepsilon_k)$ bias that vanishes only as $\varepsilon_k \rightarrow 0$ during training.

Proof. A complete proof is provided in Appendix A. □

Two practical implications follow. First, under exact barrier maximization an envelope effect holds: BPTT does not introduce spurious $\partial_x(\pi, C)$ terms in the costate recursion; the derivative of the maximized stagewise objective reduces to $\partial_x \tilde{\mathcal{H}}_{\text{bar}}$ up to discretization error. Second, with activation-only feasibility the same structure holds approximately, with an $O(\varepsilon_k)$ bias; as training progresses and ε_k shrinks, the discrete recursion converges to the PMP BSDE. This justifies using (27)–(28) as principled, low-variance policy gradients under the stated conditions.

In practice, one simply calls `.backward()` in a modern autodiff framework (e.g., PyTorch): because feasibility is encoded via smooth activations or a barrier subproblem, the rollout graph is differentiable end-to-end. For exact stagewise maximization (barrier microproblem), the resulting adjoints coincide with the constrained PMP costates up to discretization; for activation-only feasibility, they approximate the PMP costates with bias controlled by ε_k .

4.3 Projected PG-DPO (P-PGDPO) via Barrier Projection

In high dimensions, accurately learning a *parametric* policy that reproduces the stagewise Pontryagin maximizer at every time-state is statistically and computationally demanding. Even with strong regularization, a single neural network must emulate a highly structured map that depends on (t, x, y) , model coefficients, and adjoints—and must do so *while* obeying feasibility. By contrast, the barrier-augmented Hamiltonian at a fixed time-state is a small, well-conditioned nonlinear program whose Newton step leverages local second-order geometry. This observation motivates a decoupling: first stabilize the adjoints and their state-derivatives with a brief warm-up, then *directly* compute deployment controls by solving the barrier microproblem in one shot. The theory below quantifies the resulting policy error and makes explicit how it decomposes into (i) warm-up suboptimality, (ii) numerical error in adjoint estimation, and (iii) the interior-point (barrier) bias.

Two-stage procedure. P-PGDPO decouples costate estimation from policy construction while remaining within the log-barrier paradigm. After a brief warm-up to stabilize adjoints, deployment controls are computed in one shot by maximizing the barrier-augmented Hamiltonian with those adjoints held fixed.

- **Stage 1 (barrier warm-up & autodiff costates).** Run PG-DPO for K_0 iterations with the barrier microproblem in the loop to stabilize the adjoints and their spatial derivatives. In practice, modern automatic differentiation (e.g., PyTorch) provides

$$\lambda_k = \frac{\partial J}{\partial X_k}, \quad \partial_x \lambda_k = \frac{\partial^2 J}{\partial X_k^2}, \quad \partial_y \lambda_k = \frac{\partial^2 J}{\partial X_k \partial Y_k},$$

by a first backward pass (for λ) and a second autograd call on λ (for spatial derivatives), along the differentiable rollout graph. Freezing (θ, ϕ) , compute Monte Carlo averages under the barrier-feasible frozen policy:

$$\widehat{\lambda}(t, x, y) \approx \frac{1}{M_{MC}} \sum_{j=1}^{M_{MC}} \lambda^{(j)}(t, x, y), \quad \partial_x \widehat{\lambda}, \partial_y \widehat{\lambda} \text{ analogously.}$$

- **Stage 2 (one-shot barrier projection).** Given $(\widehat{\lambda}, \partial_x \widehat{\lambda}, \partial_y \widehat{\lambda})$, obtain the deployment controls at (t, x, y) by directly maximizing the barrier Hamiltonian (21) with those adjoint inputs held fixed:

$$(\pi^{\text{bar}}(t, x, y), C^{\text{bar}}(t, x, y), \eta^{\text{bar}}(t, x, y)) = \arg \max_{\pi, C, \eta} \widetilde{\mathcal{H}}_{\text{bar}}(t, x, y; \pi, C, \eta).$$

Theorem 3 (Policy-gap bound for P-PGDPO under barrier projection). *Assume the barrier-augmented Hamiltonian $\widetilde{\mathcal{H}}_{\text{bar}}$ in (21) is C^2 and strongly concave in π on the feasible interior with modulus $\mu_{\text{bar}} > 0$, LICQ holds for the active constraints, and strict interior feasibility is maintained (e.g., $\Gamma_j(\pi, C) \geq c\epsilon$ with $c > 0$). Let ε denote the Pontryagin FOC residual (in an $L^{q,p}$ -norm) of the warm-up policy (Stage 1), and let*

$$\delta_{\text{BPTT}} \equiv \kappa_1 \Delta t + \kappa_2 / \sqrt{M}$$

collect the time-discretization and Monte Carlo errors in the autodiff costates. Then, for the one-shot barrier projection in Stage 2,

$$\|\pi^{\text{bar}} - \pi^{\star}\|_{L^{q,p}} \leq C_{\text{bar}} (\varepsilon + \delta_{\text{BPTT}} + \epsilon),$$

where C_{bar} depends on model coefficients and on (μ_{bar}, c) but not on $\varepsilon, \Delta t, M$. Moreover, the instantaneous Hamiltonian gap satisfies

$$0 \leq \mathcal{H}(\pi^*, \cdot) - \mathcal{H}(\pi^{\text{bar}}, \cdot) \leq \frac{L_{\text{bar}}}{2} \|\pi^{\text{bar}} - \pi^*\|^2 = O(\varepsilon^2 + \delta_{\text{BPTT}}^2 + \epsilon^2),$$

with a Lipschitz constant L_{bar} on $\nabla_{\pi} \tilde{\mathcal{H}}_{\text{bar}}$. Hence, as the warm-up FOC gap $\varepsilon \rightarrow 0$, the discretization and MC errors $\Delta t \rightarrow 0$, $M \rightarrow \infty$, and the barrier parameter $\epsilon \rightarrow 0$, the P-PGDPO policy π^{bar} converges to the constrained PMP optimum π^* .

Proof. See Appendix B. □

Corollary 1 (Consistency and rate separation). *Under the assumptions of Theorem 3, if $\varepsilon \rightarrow 0$, $\Delta t \rightarrow 0$, $M \rightarrow \infty$, and $\epsilon \rightarrow 0$, then $\pi^{\text{bar}} \rightarrow \pi^*$ in $L^{q,p}$, and the instantaneous Hamiltonian gap vanishes at rate $O(\varepsilon^2 + \delta_{\text{BPTT}}^2 + \epsilon^2)$. Moreover, for fixed computational budget, the barrier bias $O(\epsilon)$ can be made dominantly small relative to the adjoint-estimation error by choosing $\epsilon \ll \varepsilon + \delta_{\text{BPTT}}$.*

Why does this theory matter in practice? First, it justifies the empirical observation that projection-based Pontryagin controls often attain high accuracy *much* earlier than a fully trained policy network: once the adjoints are stabilized, the stagewise Newton solve recovers the local maximizer regardless of the policy class’s approximation limits. Second, it isolates the three error sources and thus provides actionable dials—warm-up quality reduces ε ; rollout step size and the number of paths control δ_{BPTT} ; and the barrier parameter tunes the interior-point bias. Third, it clarifies the role of strong concavity and LICQ: these are precisely the conditions that make the stagewise map from adjoints to controls *well-conditioned*, ensuring stable and fast solves at scale. *Formally, this third theoretical result extends the unconstrained rate/result in Huh et al. (2025, Thm. 4) to activation/barrier-constrained portfolios, by establishing the same decomposition and rates in the presence of policy constraints.*

No network forward pass is needed at deployment beyond providing the warm-up adjoint estimates: the Newton system is $(n+2)$ -dimensional and well-conditioned by the diagonal barrier term, so the solve is extremely fast even at large n . By §3.3, using a small ϵ yields $O(\epsilon)$ policy error and $O(\epsilon^2)$ instantaneous Hamiltonian gap relative to the fully constrained PMP policy. In summary, both PG-DPO and P-PGDPO enforce feasibility solely via the log barrier; the difference is operational. PG-DPO keeps the policy in the loop and lets learning absorb the structure; P-PGDPO *extracts* the structure and uses it directly at deployment, with transparent error control through $(\varepsilon, \delta_{\text{BPTT}}, \epsilon)$.

5 Constrained Experiments: Short-Sale Ban and Consumption Cap

We evaluate PG-DPO under two practically important classes of constraints: a *short-sale ban* on risky weights and a *consumption cap* specified as a fixed fraction of wealth. In all experiments we compare the baseline policy-learning variant (“PG-DPO”) with a *manifold-projection* variant (“P-PGDPO”) that projects the stagewise controls onto the Pontryagin/KKT manifold induced by the current adjoints while enforcing feasibility via an interior-point barrier. Unless otherwise noted, feasibility is enforced either by smooth activation maps or by solving a small barrier micropersonal problem at each stage. We report root-mean-square error (RMSE) of the risky-weight vector u against a Pontryagin/KKT reference at each time-state and visualize pooled distributions of u using empirical CDFs (ECDFs). Section 5.1 covers the short-sale constraint; Section 5.2 considers the consumption cap.

Table 1: No short-selling (nonnegative orthant, floating cash): RMSE of risky-weight vector u versus the Pontryagin/KKT reference (lower is better).

| d | PG-DPO | P-PGDPO |
|----------|---------------|----------------|
| 2 | 0.017035 | 0.002509 |
| 10 | 0.079714 | 0.001251 |
| 100 | 0.011093 | 0.003015 |

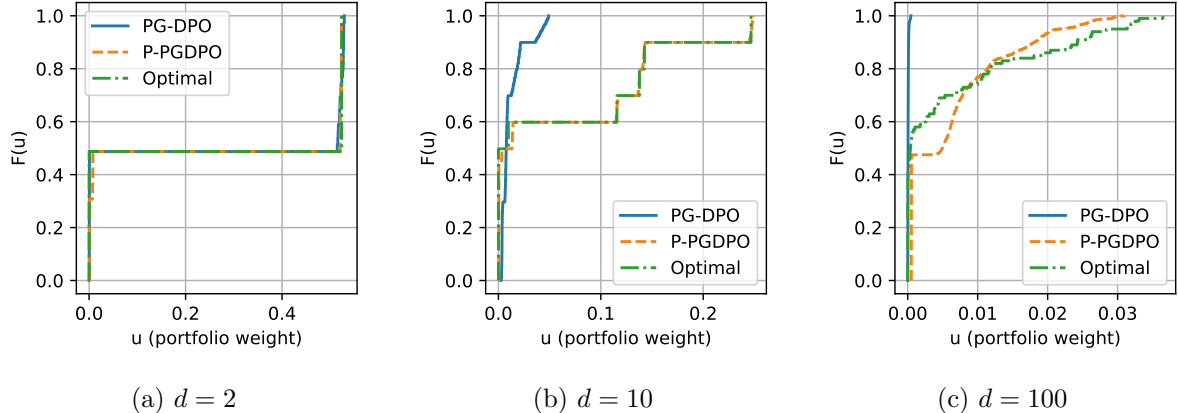


Figure 1: No short-selling: ECDFs of pooled risky weights u (over time and assets) for PG-DPO, P-PGDPO (manifold projection), and the reference policy. Closer overlap with the reference ECDF implies more accurate recovery of the target u -control.

5.1 Short-Sale Constraint (No Shorting)

We impose a no-short-sale constraint by restricting risky weights to the nonnegative orthant,

$$u_i \geq 0 \quad (i = 1, \dots, d),$$

without imposing full-investment equality; the cash share $1 - \sum_{i=1}^d u_i$ is free to float. This setting captures mandate- or regulation-driven prohibitions of short positions while allowing residual cash.

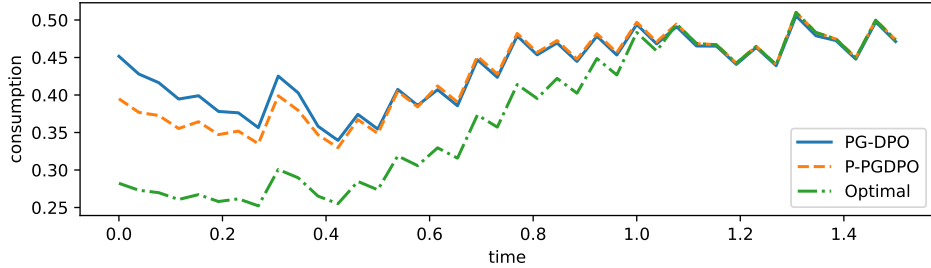
Table 1 reports the RMSE of u across dimensions $d \in \{2, 10, 100\}$. The manifold-projection variant (P-PGDPO) dominates the baseline at all scales, reducing u -RMSE by roughly 85% for $d = 2$, 98% for $d = 10$, and 73% for $d = 100$. The gains are especially pronounced at moderate and high dimension, which is consistent with activation-only feasibility leaving an ϵ -stationarity bias in the Hamiltonian FOC that becomes harder to extinguish as d grows, whereas the barrier-based projection directly recovers the stagewise Pontryagin maximizer on the feasible manifold and benefits from diagonal barrier curvature.

Figure 1 compares ECDFs of pooled risky weights (over time and assets) for PG-DPO, P-PGDPO, and a reference policy. The ECDF summarizes how allocation mass is distributed across assets and time—which asset is bought how much and how often. Closer alignment to the analytic benchmark (closed-form u_{cf} in the unconstrained limit or its constrained Pontryagin/KKT projection u_{pp}) indicates that the learned controller is recovering the *right u-control*. The manifold-projection variant closely tracks the reference over the whole support, including tails, whereas the baseline accumulates heavier mass away from the optimal tails as d increases. This distributional agreement complements the RMSE comparison and shows that projection onto the Pontryagin/KKT manifold aligns not just averages but the entire law of u .

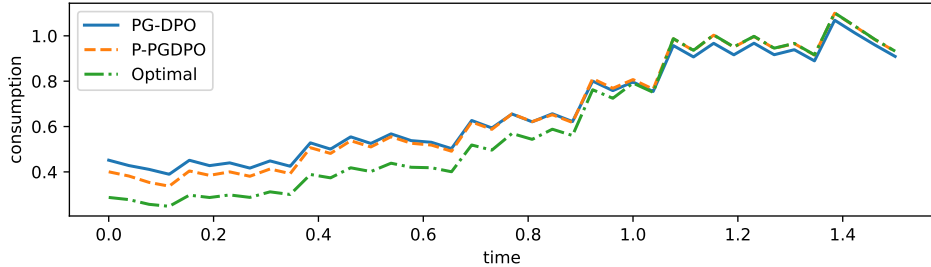
Overall, under orthant constraints with floating cash, the manifold-projection scheme consistently recovers the constrained Pontryagin/KKT policy with near-reference accuracy even in

Table 2: Consumption cap $0 \leq C_t \leq \bar{m}X_t$: RMSE (lower is better) for risky weights u (left) and consumption C (right).

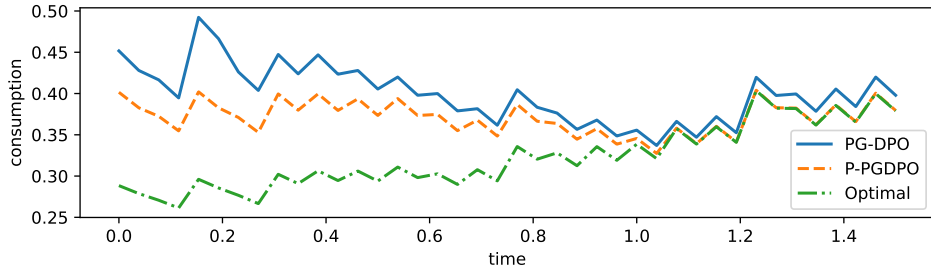
| (a) u -RMSE | | | (b) C -RMSE | | |
|---------------|---------------|----------------|---------------|---------------|----------------|
| d | PG-DPO | P-PGDPO | d | PG-DPO | P-PGDPO |
| 2 | 0.033858 | 0.000321 | 2 | 0.234102 | 0.188612 |
| 10 | 0.055776 | 0.000313 | 10 | 0.225106 | 0.188153 |
| 100 | 0.038807 | 0.000518 | 100 | 0.223304 | 0.188417 |



(a) $d = 2$



(b) $d = 10$



(c) $d = 100$

Figure 2: Consumption paths under the cap $C_t \leq \bar{m}X_t$ for PG-DPO, P-PGDPO (manifold projection), and the reference policy. P-PGDPO is uniformly closer to the reference and reduces boundary over/undershoot, but it is *not* exact: residual deviations remain near binding times and turning points.

high dimension, while activation-only learning exhibits residual bias that widens with d .

5.2 Consumption Cap (as a Fraction of Wealth)

We impose a pointwise consumption cap of the form

$$0 \leq C_t \leq \bar{m}X_t,$$

with fixed $\bar{m} \in (0, 1)$. Feasibility is enforced either by a smooth activation mapping the consumption logit into $[0, \bar{m}X_t]$ or by solving a small barrier microproblem and *projecting the stagewise control onto the Pontryagin/KKT manifold*. Although the consumption control C is scalar—hence we should not expect the same magnitude of gains as in the high-dimensional portfolio block—the consumption decision is *jointly* optimized with the portfolio weights. In practice, sharpening the u -control via manifold projection stabilizes the stagewise Hamiltonian where the cap binds and propagates to more stable consumption near the boundary.

Table 2 summarizes RMSE for both risky weights and consumption across $d \in \{2, 10, 100\}$. The manifold-projection variant reduces u -RMSE by almost two orders of magnitude for all d , while the improvement in C -RMSE is about 15–19% relative to the baseline. This disparity is expected: the consumption block is one-dimensional and frequently operates near a hard upper bound, so the available numerical headroom is structurally smaller than for high-dimensional u . Nonetheless, because the first-order conditions for C couple to π through the Hamiltonian, a more accurate recovery of the stagewise maximizer in the u -block still reduces both bias and variance in C .

Figure 2 displays representative consumption trajectories under the cap. Across all dimensions, the manifold-projection variant hugs the reference path more tightly and exhibits visibly smaller over- and undershoots near the upper boundary, whereas the baseline shows larger boundary-layer deviations that persist as d increases. At the same time, the consumption paths do *not* fully coincide with the optimal reference: small residual gaps remain—especially when the cap becomes binding and around turning points—reflecting the one-dimensional nature of C , the kink introduced by the cap, and finite barrier/adjoint estimation errors.

In summary, even though the consumption control is one-dimensional and therefore shows smaller relative gains than the high-dimensional u -block, projecting onto the Pontryagin/KKT manifold at the stage level still delivers material benefits by resolving the joint (π, C) maximization under constraints. The overall advantage of the manifold-projected PG-DPO thus grows primarily through the u -block as dimension increases, with stable but deliberately modest improvements on C near the binding boundary.

6 Conclusion

We presented a Pontryagin-guided, policy-centric framework for *constrained* dynamic portfolio choice that scales to *high-dimensional* asset universes without value-function grids. Building on the unconstrained gradient-PMP core of Huh et al. (2025), we (i) enforce all inequalities via a log-barrier microproblem solved at each time-state and (ii) introduce a *manifold-projection* variant (P–PGDPO) that projects controls onto the Pontryagin/KKT manifold given stabilized adjoints. Theoretical results establish a barrier-KKT correspondence with first-order policy accuracy ($O(\epsilon)$) and an $O(\epsilon^2)$ instantaneous Hamiltonian gap, a BPTT-PMP correspondence under activation/barrier constraints, and a clean policy-gap decomposition for manifold projection into warm-up optimality, discretization/Monte Carlo, and barrier bias.

Empirically, two canonical constraint families illustrate why the approach is particularly effective *as dimension grows*. Under a no-short constraint with *floating cash* (nonnegative orthant), manifold projection consistently recovers the constrained Pontryagin/KKT policy and sharply lowers risky-weight errors across d (Table 1); ECDFs match the reference over the full support (Figure 1), indicating recovery of the *right u-control*, not just its average. With a wealth-proportional consumption cap ($0 \leq C_t \leq \bar{m}X_t$), projection again improves accuracy and reduces boundary over/undershoot in paths (Table 2, Figure 2). As expected for a *one-dimensional* control operating near a kinked boundary, gains on C are modest (about 15–19% in RMSE) relative to the high-dimensional u -block, yet the joint (π, C) maximization is stabilized where the cap binds. Small residual gaps in C around binding times/turning points are consistent with finite barrier and adjoint-estimation errors and the cap-induced non-smoothness.

A key advantage is robustness *when classical solutions are unavailable*. Even if constrained closed-form policies are unknown—or classical optimality may fail under pathological caps or interacting constraints—the barrier central path yields well-defined, feasible *surrogate* controls with monotone Hamiltonian ascent and explicit error knobs. This makes the method a practical default precisely in regimes where DP grids are intractable and analytic solutions are unavailable.

Looking ahead, we expect the benefits to be *even stronger when the investment opportunity set is not constant* (time-varying or stochastic drifts/volatilities, factor or regime dynamics), a regime in which classical closed-form benchmarks are scarce and the structure of constrained optima is often unknown. In such nonstationary settings the local, stagewise barrier solve remains lightweight while value-based methods deteriorate rapidly with state/action growth. Immediate extensions include transaction costs, leverage/sector limits, and path-dependent rules (e.g., ratcheting) via barrier terms and state augmentation; incomplete-information and robust/distributionally-robust variants via modified Hamiltonian drivers; and algorithmic refinements such as adaptive barrier schedules, primal-dual projections, and variance-reduced adjoint estimators.

Overall, projecting onto the Pontryagin/KKT manifold enables accurate, scalable, and constraint-respecting policies in high dimensions, remains effective when classical solutions are unknown or do not exist, and is poised to deliver larger gains in realistically *time-varying* investment environments.

Acknowledgments

This work was supported by the National Research Foundation of Korea (NRF) grant funded by the Korea government (MSIT) (RS-2024-00355646 and NRF-2022R1F1A1063371).

References

- Baldazzi, P. & Lynch, A. W. (1999). Transaction costs and predictability: Some utility cost calculations. *Journal of Financial Economics*, 52(1), 47–78. 1
- Bertsekas, D. P. (1997). Nonlinear programming. *Journal of the Operational Research Society*, 48(3), 334–334. 3.2, 3.2
- Boyd, S. (2004). Convex optimization. *Cambridge UP*. 3.2, 3.2
- Brandt, M. W., Goyal, A., Santa-Clara, P., & Stroud, J. R. (2005). A simulation approach to dynamic portfolio choice with an application to learning about return predictability. *The Review of Financial Studies*, 18(3), 831–873. 1
- Buraschi, A., Porchia, P., & Trojani, F. (2010). Correlation risk and optimal portfolio choice. *The Journal of Finance*, 65(1), 393–420. 1
- Campbell, J. Y., Chan, Y. L., & Viceira, L. M. (2003). A multivariate model of strategic asset allocation. *Journal of financial economics*, 67(1), 41–80. 1
- Campbell, J. Y. & Viceira, L. M. (1999). Consumption and portfolio decisions when expected returns are time varying. *The Quarterly Journal of Economics*, 114(2), 433–495. 1
- Campbell, J. Y. & Viceira, L. M. (2001). Who should buy long-term bonds? *American Economic Review*, 91(1), 99–127. 1
- Constantinides, G. M. (1990). Habit formation: A resolution of the equity premium puzzle. *Journal of political Economy*, 98(3), 519–543. 1, 2.2

- Cvitanić, J. & Karatzas, I. (1996). Hedging and portfolio optimization under transaction costs: A martingale approach 1 2. *Mathematical finance*, 6(2), 133–165. 1, 2.2
- Dai, M., Dong, Y., Jia, Y., & Zhou, X. Y. (2023). Learning merton's strategies in an incomplete market: Recursive entropy regularization and biased gaussian exploration. *arXiv preprint arXiv:2312.11797*. 1
- Dybvig, P. H. (1995). Dusenberry's ratcheting of consumption: optimal dynamic consumption and investment given intolerance for any decline in standard of living. *The Review of Economic Studies*, 62(2), 287–313. 1, 2.2
- Fleming, W. H. & Soner, H. M. (2006). *Controlled Markov processes and viscosity solutions*, volume 25. Springer Science & Business Media. 1, 2.2, 2.2, 3.1, 3.2
- Garlappi, L. & Skoulakis, G. (2010). Solving consumption and portfolio choice problems: The state variable decomposition method. *The Review of Financial Studies*, 23(9), 3346–3400. 1
- Han, J., Jentzen, A., & E, W. (2018). Solving high-dimensional partial differential equations using deep learning. *Proceedings of the National Academy of Sciences*, 115(34), 8505–8510. 1
- Huh, J., Jeon, J., & Koo, H. K. (2025). Breaking the dimensional barrier: A pontryagin-guided direct policy optimization for continuous-time multi-asset portfolio. *arXiv preprint arXiv:2504.11116*. 1, 4, 4.2, 4.3, 6
- Jurek, J. W. & Viceira, L. M. (2011). Optimal value and growth tilts in long-horizon portfolios. *Review of Finance*, 15(1), 29–74. 1
- Karatzas, I., Lehoczky, J. P., & Shreve, S. E. (1987). Optimal portfolio and consumption decisions for a "small investor" on a finite horizon. *SIAM journal on control and optimization*, 25(6), 1557–1586. 1, 2.2
- Karatzas, I. & Shreve, S. E. (1998). *Methods of Mathematical Finance*. New York: Springer. 1, 2.2
- Kim, T. S. & Omberg, E. (1996). Dynamic nonmyopic portfolio behavior. *The Review of Financial Studies*, 9(1), 141–161. 1
- Liu, J. (2007). Portfolio selection in stochastic environments. *The Review of Financial Studies*, 20(1), 1–39. 1
- Lynch, A. W. (2001). Portfolio choice and equity characteristics: Characterizing the hedging demands induced by return predictability. *Journal of Financial Economics*, 62(1), 67–130. 1
- Lynch, A. W. & Balduzzi, P. (2000). Predictability and transaction costs: The impact on rebalancing rules and behavior. *The Journal of Finance*, 55(5), 2285–2309. 1
- Merton, R. C. (1969). Lifetime portfolio selection under uncertainty: The continuous-time case. *The review of Economics and Statistics*, (pp. 247–257). 1, 2
- Merton, R. C. (1971). Optimum consumption and portfolio rules in a continuous-time model. *Journal of Economic Theory*, 3(4), 373–413. 1, 2
- Nesterov, Y. & Nemirovskii, A. (1994). *Interior-point polynomial algorithms in convex programming*. SIAM. 3.2, 3.2
- Nocedal, J. & Wright, S. J. (2006). *Numerical optimization*. Springer. 3.2, 3.2

- Pardoux, E. & Peng, S. (1990). Adapted solution of a backward stochastic differential equation. *Systems & control letters*, 14(1), 55–61. 3.1
- Pham, H. (2009). *Continuous-time stochastic control and optimization with financial applications*, volume 61. Springer Science & Business Media. 1, 3.1
- Pontryagin, L. S. (2018). *Mathematical theory of optimal processes*. Routledge. 3.1
- Raissi, M., Perdikaris, P., & Karniadakis, G. E. (2019). Physics-informed neural networks: A deep learning framework for solving forward and inverse problems involving nonlinear partial differential equations. *Journal of Computational physics*, 378, 686–707. 1
- Samuelson, P. A. (1969). Lifetime portfolio selection by dynamic stochastic programming. *The Review of Economics and Statistics*, 51(3), 239–246. 1
- Shreve, S. E. & Soner, H. M. (1994). Optimal investment and consumption with transaction costs. *The Annals of Applied Probability*, (pp. 609–692). 1, 2.2, 3.2
- Sundaresan, S. M. (1989). Intertemporally dependent preferences and the volatility of consumption and wealth. *Review of financial Studies*, 2(1), 73–89. 1, 2.2
- Wächter, A. & Biegler, L. T. (2006). On the implementation of an interior-point filter line-search algorithm for large-scale nonlinear programming. *Mathematical programming*, 106(1), 25–57. 3.2
- Weinan, E. (2017). A proposal on machine learning via dynamical systems. *Communications in Mathematics and Statistics*, 1(5), 1–11. 1
- Wright, S. J. (1997). *Primal-dual interior-point methods*. SIAM. 3.2, 3.2, 3.2

A Proof of Theorem 2

We collect basic regularity and feasibility assumptions used below.

Assumption 2 (Regularity and feasibility). *On the training domain, model coefficients $(\tilde{\mu}, \tilde{V})$ are bounded and C^1 in x , the marginal utility U' is locally Lipschitz on the image of C_ϕ , and the policy (π_θ, C_ϕ) is C^1 and bounded. Feasibility at each time–state is enforced either by an exact barrier micropoproblem whose maximizer (π_k, C_k, η_k) is computed at every step, or by smooth activations that map logits to the feasible set; in the latter case, the stagewise control is ε_k -stationary for the barrier-augmented Hamiltonian with $\epsilon \rightarrow 0$, i.e. $\|\nabla_{\pi, C} \tilde{\mathcal{H}}_{\text{bar}}\| \leq \varepsilon_k$ with $\sum_k \varepsilon_k \Delta t = O(\varepsilon)$.*

The exponential–Euler wealth update used in the main text admits the Euler–Maruyama representation

$$X_{k+1} = X_k + b_k \Delta t + \sigma_k \cdot \Delta W_k + r_k^{(X)}, \quad b_k := X_k \pi_k^\top \tilde{\mu}_k - C_k, \quad \sigma_k := X_k \pi_k^\top \tilde{V}_k, \quad (29)$$

where the remainder $r_k^{(X)}$ satisfies $\mathbb{E} \left[|r_k^{(X)}| \mid \mathcal{F}_{t_k} \right] \leq c \Delta t^{3/2}$ for some constant $c > 0$. In what follows, derivatives with respect to x act on the explicit x -dependence of b and σ , while the realized controls (π_k, C_k) are treated as fixed inputs at each stage (policy-fixed envelope view).

We shall use the standard envelope identity for the stagewise maximization.

Lemma 3 (Envelope at the stagewise maximizer). *Fix $(t_k, X_k, Y_k, \lambda_{k+1}, Z_{k+1})$. If (π_k, C_k, η_k) maximizes $\tilde{\mathcal{H}}_{\text{bar}}(t_k, x, Y_k; \pi, C, \eta, \lambda_{k+1}, Z_{k+1})$ at $x = X_k$, then*

$$\frac{\partial}{\partial x} \left[\max_{\pi, C, \eta} \tilde{\mathcal{H}}_{\text{bar}}(t_k, x, Y_k; \pi, C, \eta, \lambda_{k+1}, Z_{k+1}) \right]_{x=X_k} = \partial_x \tilde{\mathcal{H}}_{\text{bar}}(t_k, X_k, Y_k; \pi_k, C_k, \eta_k, \lambda_{k+1}, Z_{k+1}).$$

If (π_k, C_k, η_k) is only ε_k -stationary, the identity holds up to an $O(\varepsilon_k)$ error.

Proof. At an interior maximizer, the derivatives of $\tilde{\mathcal{H}}_{\text{bar}}$ with respect to (π, C, η) vanish, so the derivative of the maximized value with respect to the parameter x equals the x -partial evaluated at the maximizer (classical envelope theorem). Under ε_k -stationarity, the nonzero residual $\nabla_{\pi, C} \tilde{\mathcal{H}}_{\text{bar}}$ contributes an $O(\varepsilon_k)$ term because $\partial_x(\pi_k, C_k)$ is bounded by regularity of the maps. \square

We now prove the theorem. Define the pathwise adjoints by

$$\lambda_k := \frac{\partial J_e}{\partial X_k}, \quad Z_{k+1} := \frac{1}{\Delta t} \mathbb{E} \left[\lambda_{k+1} \Delta W_k^\top \mid \mathcal{F}_{t_k} \right] \in \mathbb{R}^n,$$

so that the martingale representation in L^2 reads $\lambda_{k+1} = \mathbb{E}[\lambda_{k+1} \mid \mathcal{F}_{t_k}] + Z_{k+1}^\top \Delta W_k$. Let $R_k := e^{-\rho t_k} U(C_k) \Delta t$ denote the stagewise contribution to the objective. By the chain rule for backpropagation-through-time and the dynamics (29),

$$\lambda_k = \frac{\partial R_k}{\partial X_k} + \mathbb{E} \left[\lambda_{k+1} \frac{\partial X_{k+1}}{\partial X_k} \mid \mathcal{F}_{t_k} \right], \quad \frac{\partial X_{k+1}}{\partial X_k} = 1 + \partial_x b_k \Delta t + \partial_x \sigma_k \cdot \Delta W_k + \rho_k^{(X)},$$

with $\mathbb{E}[\rho_k^{(X)} \mid \mathcal{F}_{t_k}] = O(\Delta t^{3/2})$. Substituting the derivative of X_{k+1} and using the martingale representation of λ_{k+1} gives

$$\lambda_k - \mathbb{E}[\lambda_{k+1} \mid \mathcal{F}_{t_k}] = \Delta t \left(\frac{1}{\Delta t} \frac{\partial R_k}{\partial X_k} + \lambda_{k+1} \partial_x b_k + (\partial_x \sigma_k) Z_{k+1} \right) + O(\Delta t^{3/2}).$$

The envelope lemma 3 eliminates the implicit $\partial_x(\pi_k, C_k)$ contributions coming from the stagewise feasible map. Indeed,

$$\frac{1}{\Delta t} \frac{\partial R_k}{\partial X_k} = \partial_x \tilde{\mathcal{H}}_{\text{bar}}(t_k, X_k, Y_k; \pi_k, C_k, \eta_k, \lambda_{k+1}, Z_{k+1}) - \lambda_{k+1} \partial_x b_k - (\partial_x \sigma_k) Z_{k+1} + O(\varepsilon_k),$$

where $\varepsilon_k \equiv 0$ if the barrier subproblem is solved exactly, and ε_k is the stationarity residual in the activation-only case (with $\epsilon \rightarrow 0$). Combining the last two displays yields the discrete backward recursion

$$\lambda_k - \mathbb{E}[\lambda_{k+1} \mid \mathcal{F}_{t_k}] = \Delta t \partial_x \tilde{\mathcal{H}}_{\text{bar}}(t_k, X_k, Y_k; \pi_k, C_k, \eta_k, \lambda_{k+1}, Z_{k+1}) + O(\Delta t^{3/2} + \varepsilon_k \Delta t).$$

Since $\lambda_{k+1} - \mathbb{E}[\lambda_{k+1} \mid \mathcal{F}_{t_k}] = Z_{k+1}^\top \Delta W_k$, we obtain the pathwise form

$$\lambda_k - \lambda_{k+1} = \Delta t \partial_x \tilde{\mathcal{H}}_{\text{bar}}(t_k, X_k, Y_k; \pi_k, C_k, \eta_k, \lambda_{k+1}, Z_{k+1}) - Z_{k+1}^\top \Delta W_k + O(\Delta t^{3/2} + \varepsilon_k \Delta t).$$

Taking conditional expectations given \mathcal{F}_{t_k} removes the martingale term and leaves

$$\mathbb{E}[\lambda_k - \lambda_{k+1} \mid \mathcal{F}_{t_k}] = \Delta t \partial_x \tilde{\mathcal{H}}_{\text{bar}}(t_k, X_k, Y_k; \pi_k, C_k, \eta_k, \lambda_{k+1}, Z_{k+1}) + O(\Delta t^{3/2} + \varepsilon_k \Delta t).$$

Under Assumption 2 and standard stability of Euler schemes for linear BSDEs with Lipschitz drivers, the piecewise-constant interpolation of (λ_k, Z_k) converges in L^2 , as $\Delta t \rightarrow 0$ and $\varepsilon \rightarrow 0$, to the unique solution (λ_t, Z_t) of

$$d\lambda_t = -\partial_x \tilde{\mathcal{H}}_{\text{bar}}(t, X_t, Y_t; \pi_t, C_t, \eta_t, \lambda_t, Z_t) dt + Z_t^\top dW_t,$$

which is precisely the Pontryagin costate BSDE for the constrained problem. This completes the proof. \square

B Proof of Theorem 3

We first collect the regularity conditions used in the proof.

Assumption 3 (Regularity for barrier projection). *On the training domain, the model coefficients are C^2 and bounded, and the barrier-augmented Hamiltonian*

$$\tilde{\mathcal{H}}_{\text{bar}}(t, x, y; \pi, C, \eta, \lambda, Z) = e^{-\rho t} U(C) + \lambda b(t, x, y; \pi, C) + Z^\top \sigma(t, x, y; \pi) + \eta (1 - \mathbf{1}^\top \pi) - \epsilon \sum_{j=1}^{m_c} \ln \Gamma_j(t, x, y; \pi, C)$$

is C^2 in (π, C) for fixed $(t, x, y, \lambda, Z, \eta, \epsilon)$, where $b = x \pi^\top \tilde{\mu} - C$ and $\sigma = x \pi^\top \tilde{V}$.

(i) (Strong concavity in π on the feasible interior) *There exists $\mu_{\text{bar}} > 0$ such that for all feasible directions d with $\mathbf{1}^\top d = 0$,*

$$-d^\top \nabla_{\pi\pi}^2 \tilde{\mathcal{H}}_{\text{bar}}(t, x, y; \pi, C, \eta, \lambda, Z) d \geq \mu_{\text{bar}} \|d\|^2.$$

(ii) (LICQ and interior feasibility) *The equality constraint $h(\pi) := \mathbf{1}^\top \pi - 1 = 0$ and the active barrier constraints satisfy LICQ at the maximizer. Moreover, strict interior feasibility holds along the central path, i.e. $\Gamma_j(\pi, C) \geq c \epsilon$ for some $c > 0$ uniformly in (t, x, y) .*

(iii) (L -smoothness) $\nabla_\pi \tilde{\mathcal{H}}_{\text{bar}}$ is L_{bar} -Lipschitz on the interior feasible set.

We will use two lemmas. The first is a sensitivity bound for the barrier maximizer with respect to perturbations in (λ, Z) and ϵ ; the second controls the perturbation of the adjoints produced by the warm-up phase.

Lemma 4 (Sensitivity of barrier maximizer). *Fix (t, x, y) and let $(\pi^{\text{bar}}, C^{\text{bar}}, \eta^{\text{bar}})$ solve*

$$(\pi^{\text{bar}}, C^{\text{bar}}, \eta^{\text{bar}}) \in \arg \max_{\pi, C, \eta} \tilde{\mathcal{H}}_{\text{bar}}(t, x, y; \pi, C, \eta, \lambda, Z) \quad \text{subject to} \quad \mathbf{1}^\top \pi = 1, \quad \Gamma_j(\pi, C) > 0,$$

for given (λ, Z, ϵ) . Under Assumption 3, there exist constants $\kappa_\lambda, \kappa_Z, \kappa_\epsilon > 0$ (depending only on model bounds and (μ_{bar}, c)) such that for any $(\lambda', Z', \epsilon')$ in a neighborhood,

$$\|\pi^{\text{bar}}(\lambda', Z', \epsilon') - \pi^{\text{bar}}(\lambda, Z, \epsilon)\| \leq \kappa_\lambda |\lambda' - \lambda| + \kappa_Z \|Z' - Z\| + \kappa_\epsilon |\epsilon' - \epsilon|.$$

Proof. Write the stagewise FOC map

$$\mathbf{F}(\pi, C, \eta; \lambda, Z, \epsilon) = \begin{pmatrix} \nabla_\pi \tilde{\mathcal{H}}_{\text{bar}}(t, x, y; \pi, C, \eta, \lambda, Z) \\ \nabla_C \tilde{\mathcal{H}}_{\text{bar}}(t, x, y; \pi, C, \eta, \lambda, Z) \\ \mathbf{1}^\top \pi - 1 \end{pmatrix} = \mathbf{0}.$$

By strong concavity in π on the tangent space $\{\mathbf{1}^\top d = 0\}$ and LICQ, the Jacobian $D_{(\pi, C, \eta)} \mathbf{F}$ at $(\pi^{\text{bar}}, C^{\text{bar}}, \eta^{\text{bar}})$ is nonsingular (block KKT matrix with a negative definite Schur complement). The implicit function theorem yields a C^1 map $(\lambda, Z, \epsilon) \mapsto (\pi^{\text{bar}}, C^{\text{bar}}, \eta^{\text{bar}})$ locally, and the desired Lipschitz bound follows by mean-value estimates with constants depending on uniform bounds and the inverse-Jacobian norm, which is controlled by (μ_{bar}, c) . \square

Lemma 5 (Adjoint stability under warm-up residual and discretization). *Let (λ^*, Z^*) denote the PMP costates along the constrained optimal policy π^* . Let the warm-up policy from Stage 1 have Pontryagin FOC residual $\varepsilon = \varepsilon$ in an $L^{q,p}$ norm, and let the autodiff adjoints be computed with time step Δt and M Monte Carlo paths. Under Lipschitz coefficients and bounded utility curvature, there exist constants $a_1, a_2 > 0$ such that the stagewise adjoint estimates $(\hat{\lambda}, \hat{Z})$ obtained in Stage 1 satisfy*

$$\|(\hat{\lambda}, \hat{Z}) - (\lambda^*, Z^*)\|_{L^{q,p}} \leq a_1 \varepsilon + a_2 (\kappa_1 \Delta t + \kappa_2 / \sqrt{M}) = a_1 \varepsilon + a_2 \delta_{\text{BPTT}}.$$

Proof. The FOC residual ε implies that the warm-up policy is $O(\varepsilon)$ -close to the stagewise maximizer of the true constrained Hamiltonian (by strong concavity, the FOC map has a Lipschitz inverse on the tangent space). Forward coefficients and the costate BSDE driver are Lipschitz in the controls; hence the resulting costates are Lipschitz in the policy (standard stability of linear BSDEs). Discretization and Monte Carlo sampling incur the additional error $\kappa_1 \Delta t + \kappa_2 / \sqrt{M}$ in $L^{q,p}$ by standard weak/strong error estimates for Euler-Maruyama and sample means. Combining the two contributions yields the bound. \square

We now prove the policy bound and the Hamiltonian gap.

Proof of Theorem 3. Fix (t, x, y) . Stage 2 computes

$$(\pi^{\text{bar}}, C^{\text{bar}}, \eta^{\text{bar}}) \in \arg \max_{\pi, C, \eta} \tilde{\mathcal{H}}_{\text{bar}}(t, x, y; \pi, C, \eta, \hat{\lambda}, \hat{Z}) \quad \text{with barrier } \epsilon > 0 \text{ held fixed.}$$

Insert and subtract the solution that would be obtained with the *true* adjoints (λ^*, Z^*) :

$$\|\pi^{\text{bar}}(\hat{\lambda}, \hat{Z}, \epsilon) - \pi^*\| \leq \underbrace{\|\pi^{\text{bar}}(\hat{\lambda}, \hat{Z}, \epsilon) - \pi^{\text{bar}}(\lambda^*, Z^*, \epsilon)\|}_{\text{(A) adjoint perturbation}} + \underbrace{\|\pi^{\text{bar}}(\lambda^*, Z^*, \epsilon) - \pi^*\|}_{\text{(B) barrier bias}}.$$

For (A), Lemma 4 with $\epsilon' = \epsilon$ gives

$$\|\pi^{\text{bar}}(\hat{\lambda}, \hat{Z}, \epsilon) - \pi^{\text{bar}}(\lambda^*, Z^*, \epsilon)\| \leq \kappa_\lambda |\hat{\lambda} - \lambda^*| + \kappa_Z \|\hat{Z} - Z^*\| \leq \kappa \|(\hat{\lambda}, \hat{Z}) - (\lambda^*, Z^*)\|,$$

and Lemma 5 bounds the last term by $a_1 \varepsilon + a_2 \delta_{\text{BPTT}}$. For (B), the barrier central-path identity implies that, as $\epsilon \downarrow 0$, the barrier maximizer converges to the KKT/PMP solution. Quantitatively, by the barrier error bound in Section 3.3, there exists $b_1 > 0$ such that

$$\|\pi^{\text{bar}}(\lambda^*, Z^*, \epsilon) - \pi^*\| \leq b_1 \epsilon.$$

Collecting (A) and (B), we obtain

$$\|\pi^{\text{bar}} - \pi^*\| \leq C_{\text{bar}} (\varepsilon + \delta_{\text{BPTT}} + \epsilon),$$

for $C_{\text{bar}} := \max\{\kappa a_1, \kappa a_2, b_1\}$, uniformly on the domain. This proves the policy bound.

For the instantaneous Hamiltonian gap, L_{bar} -smoothness of $\nabla_\pi \tilde{\mathcal{H}}_{\text{bar}}$ on the feasible interior yields

$$0 \leq \mathcal{H}(\pi^*, \cdot) - \mathcal{H}(\pi^{\text{bar}}, \cdot) \leq \frac{L_{\text{bar}}}{2} \|\pi^{\text{bar}} - \pi^*\|^2 = O(\varepsilon^2 + \delta_{\text{BPTT}}^2 + \epsilon^2),$$

where we used that $\tilde{\mathcal{H}}_{\text{bar}}$ and \mathcal{H} have the same π -quadratic modulus on the interior (the barrier contributes only a diagonal curvature term that is controlled uniformly by interior feasibility and ϵ), and the last equality follows from the already established policy bound. Finally, letting $\varepsilon \rightarrow 0$, $\Delta t \rightarrow 0$, $M \rightarrow \infty$, and $\epsilon \rightarrow 0$ shows $\pi^{\text{bar}} \rightarrow \pi^*$, as claimed. \square